

Epsilon Near Zero (ENZ) Based Kagome Photonic Crystal Fiber for Low Loss, High Birefringence and Near Zero Flat Dispersion in THz Regime

Sayed Asaduzzaman

Rangamati Science and Technology University

Hasin Rehana

Rajshahi University of Engineering and Technology

M. D. Tanzil Aziz

Ahsanullah University of Science and Technology

Osama S. Faragallah

Taif University

Mohammed Baz

Taif University

Mahmoud M. A. Eid

Taif University

ahmed nabuh zaki rashed (✉ ahmed_733@yahoo.com)

Menoufia University <https://orcid.org/0000-0002-5338-1623>

Research Article

Keywords: Kagome PCF, ENZ Material, High Birefringence, Confinement loss, Material Loss, Flat Dispersion

Posted Date: July 1st, 2021

DOI: <https://doi.org/10.21203/rs.3.rs-599601/v1>

License: © ⓘ This work is licensed under a Creative Commons Attribution 4.0 International License.

[Read Full License](#)

Epsilon Near Zero (ENZ) Based Kagome Photonic Crystal Fiber for Low Loss, High Birefringence and Near Zero Flat Dispersion in THz Regime

Sayed Asaduzzaman¹, Hasin Rehana², M. D. Tanzil Aziz³, Osama S. Faragallah⁴, Mohammed Baz⁵, Mahmoud M. A. Eid⁶, Ahmed Nabih Zaki Rashed^{7,*}

¹Department of Computer Science and Engineering, Rangamati Science and Technology University, Rangamati, Bangladesh

Email: s.asaduzzaman.bd@ieee.org

²Department of Computer Science and Engineering, Rajshahi University of Engineering and Technology (RUET), Rajshahi, Bangladesh

Email: hasin.cse13@gmail.com

³Department of Electrical and Electronic Engineering (EEE), Ahsanullah University of Science and Technology (AUST), Dhaka, Bangladesh

E-mail: Tanjilaziz1212@gmail.com

⁴Department of Information Technology, College of Computers and Information Technology, Taif University, P.O. Box 11099, Taif 21944, Saudi Arabia

Email: o.salah@tu.edu.sa

⁵Department of Computer Engineering, College of Computers and Information Technology, Taif University, P.O. Box 11099, Taif 21944, Saudi Arabia

Email: mo.baz@tu.edu.sa

⁶Department of Electrical Engineering, College of Engineering, Taif University, P.O. Box 11099, Taif 21944, Saudi Arabia

E-mail: m.elfateh@tu.edu.sa

⁷Electronics and Electrical Communications Engineering Department, Faculty of Electronic Engineering, Menouf 32951, Menoufia University, Egypt

*Corresponding Author: ahmed_733@yahoo.com

Abstract

In this research, we have proposed two novel types of Kagome PCFs one is slotted core PCF (S-KPCF) and another one is circular PCF (C-KPCF). FEM has been applied with boundary condition to investigate the optical properties of Proposed PCFs. HRS material along with Epsilon Near Zero (ENZ) material has been applied in core and TOPAS was used as background material. Numerical investigation takes place a wider frequency range for 0.8 THz to 2 THz. Slotted core PCF (S-KPCF) shows eminent birefringence of 2.98×10^{-2} , Lower EML of 0.232 cm^{-1} , lower confinement loss of 2.76×10^{-8} , Bending loss 10.76×10^{-9} , Total loss of 0.232 cm^{-1} at frequency 1THz. Besides circular core PCF (C-KPCF) shows eminent birefringence of 8.69×10^{-2} , Lower effective material loss of 0.746 cm^{-1} , lower confinement loss of 2.80×10^{-7} , Bending loss 7.76×10^{-9} , Total loss of 0.746 cm^{-1} at 1THz. Both PCFs show flat dispersion near zero (for S-KPCF is -0.997 ps/nm/Km and for C-KPCF is -0.797 ps/nm/Km) range. V-Parameter of both of the PCF indicates that both PCF is multimode PCF. Comparison of the proposed PCFs shows that C-KPCF shows better results than S-KPCF and both PCFs shows better results than previous PCFs.

Keywords: Kagome PCF; ENZ Material; High Birefringence; Confinement loss; Material Loss; Flat Dispersion

I. Introduction

Now-a-Days for THz applications Photonic Crystal Fibers (PCF) has been widely used [1,2]. Due to the functioning advantages like structural flexibility, tunability of dispersion, low loss of Photonic Crystal Fibers has been positioned in optical regime [3]. In recent years for THz applications three types of PCFs are being used. Photonic Band Gap properties based wave guiding principles for Hollow core PCF is one kind [4]. Second kind of PCF is a solid core PCF where total internal reflection principle based wave guiding properties is present [5]. Porous fiber PCF is third kind of PCF which is also based on total internal reflection (TIR). To concentrate field energy at core region and diminishing propagation loss in porous fiber PCF additional sub wavelength lay out of air holes brought in in core [6].

Elliptical air holes at both core and cladding region based photonic crystal fiber have been suggested by Kim et al. [7]. The suggested PCF shows higher birefringence of 10^{-2} and negative flat dispersion at the same time. Epsilon Near Zero (ENZ) material based Hexagonal PCF was proposed in [8] which was numerically investigated where high birefringence has been achieved. In [9] Habib et al. suggested an elliptical hole based core and decagonal cladding PCF that depicts negative flat dispersion of -558.96 ps/nm/km and birefringence of 0.0299. In the year of 2017, M. A. Habib et al. proposed a PCF whose cladding was rectangular and core is asymmetrical slotted core. The Proposed PCF shows high confinement loss whereas a lower EML of 0.035 cm^{-1} [10]. Rectangular air holes based slotted core PCF was presented in [11] that exhibits EML of 0.047 cm^{-1} . S. Rana et al. proposed a Kagome shaped cladding with hexagonal core based PCF which demonstrates EML of 0.029 cm^{-1} at 1.3 THz [12].

Hexagonal Porous core rotated hexagonal based PCF has been shown in [13]. The PCF shows EML of 0.43 dB/cm and higher birefringence of 0.033. In [14] a rectangular slotted core and slotted cladding Photonic crystal fiber has been illustrated which shows low dispersion 0.5 ps/THz/cm and low material absorption loss of $0.0103\text{-}0.0145 \text{ cm}^{-1}$. Circular air holes based PCF with high birefringence has been shown in [15]. Optical properties like confinement loss 10^{-3} dB/m , eminent birefringence of 0.033 and effective material loss of 0.43 dB/cm has been gained in [13] where PCF was porous core

hexagonal shaped. Asymmetric rectangular or elliptical hole PCF shows higher birefringence than the circular holes. EML of 0.08 cm^{-1} and high birefringence 0.045 gained for multihole core PCF in [16].

In this research, we have proposed two Kagome PCFs with different core formation. One PCF is elliptical and rectangular hole based slotted core Kagome PCF and another one is circular hole in hexagonal formation based core Kagome PCF. We have investigated the optical properties by tuning the geometry of the PCFs. Our proposed PCF shows better results in term of Dispersion, Birefringence, confinement loss, bending loss, effective material loss, total loss and V-parameters. The results have also been compared with previous papers. The structural design has been described and numerical results have also been described in this paper.

II. Proposed Kagome PCF Design Methodology

Here we have proposed two Kagome Photonic Crystal Fiber with different core formation which has been shown in Fig 1(a) and Fig 1(b). Kagome PCF with slotted hole based core is defined as PCF1 or Slotted Kagome PCF (S-KPCF) and another Kagome PCF with circular hole based core is defined as Circular Kagome PCF2 (C-KPCF). For both of the PCF background material was set a polymer named TOPAS whose refractive index is constant ($n_{\text{TOPAS}}=1.53$). At the core region we have used two types of material one is Epsilon Near Zero (ENZ) ($n_{\text{ENZ}}=0.1$) and another one is High resistivity silicon (HRS) ($n_{\text{HRS}}=3.41$). Core region of the PCF1 or S-KPCF is organized with 3 elliptical slots at the center and 6 rectangular slots. 3 elliptical slots are filled with HRS material and other 6 rectangular slots filled with ENZ materials.

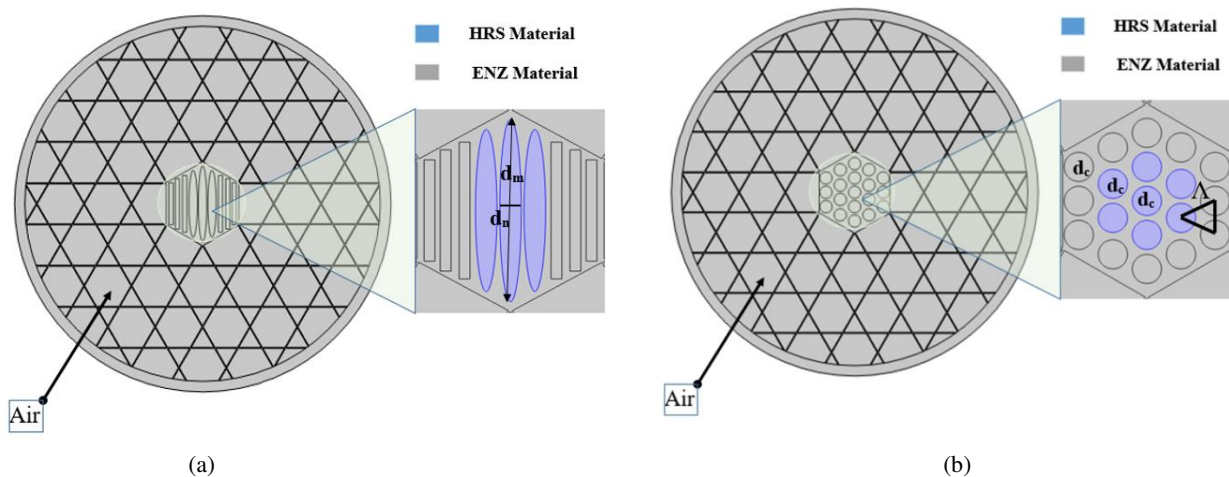
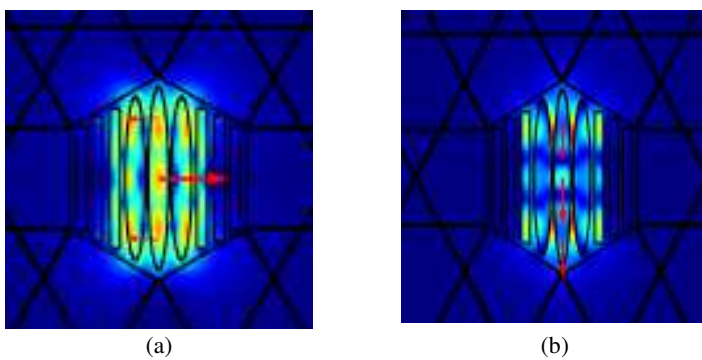


Fig 1: Ends Face View of the Proposed (a) S-KPCF (b) C-KPCF with magnification of core.

The ratio of the 3 elliptical slots are kept same which is denoted by $\eta_1 = (d_n/d_m)$ where d_m and d_n are major and minor axis. Moreover, Core region of the PCF2 or C-KPCF is formed with circular holes in hexagonal formation. The diameter of core holes are denoted by d_c and pitch (from center to another center distance of neighboring holes) is denoted by Λ . The ratio of diameter and pitch is denoted by $\eta_2 = (d_c/\Lambda)$. Cladding area is formed by Kagome formation where the holes are filled with air.

III. Simulation Results and Discussion

State of the Art Finite Element Method (FEM) based COMSOL Multiphysics has been applied to numerically calculate guiding properties. PML (Perfectly Matched layer) boundary condition was employed in the proposed PCFs to compute leakage loss or confinement loss. Fig 2 (a), (b), (c), (d) shows the mode field distribution at core region for proposed PCF1 (S-KPCF) and PCF2 (C-KPCF) along X-axis and Y-Axis. Figure 2 shows that the fundamental mode is nicely confined at core region.



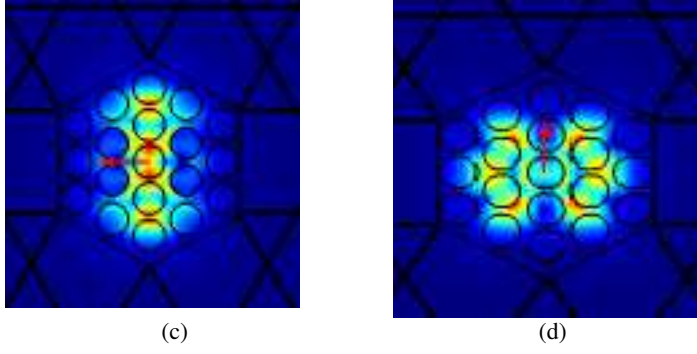


Fig. 2: Electric field distribution of the proposed Kagome PCF1 (S-KPCF) (a) X-Axis (b) Y-Axis and PCF2 (C-KPCF) (a) X-Axis (b).

A) Birefringence

The deviation between effective index along X-axis (n_x) and Y-Axis (n_y) is Birefringence which has been defined in Eq(1) [17]. Fig 3 shows the birefringence graph versus Frequency (THz) for Proposed PCFs PCF1 (S-KPCF) and PCF2 (C-KPCF). For both of the PCF birefringence curve is different. For PCF1 gains with the increase of Frequency from 0.8 THz to 1.2 THz and then the birefringence curve is almost flat upto 2 THz. For PCF2 we get higher birefringence than PCF1. For PCF2 the birefringence decreases at a constant rate from 0.8 THz to 2 THz. The ratio between major and minor axis is denoted by η_1 that has been varied ($\eta_1=0.80, \eta_1=0.70, \eta_1=0.60$) and illustrated in Fig 4. For $\eta_1=0.80$ higher birefringence show than the other variations for PCF1. The core air hole diameter and pitch ratio has been denoted by η_2 in PCF2. The ratio η_2 has been varied and the results show in the Fig 5. The variation takes place to optimize the structure. Variation for air filling ratio are ($\eta_i=0.571, \eta_i=0.490, \eta_i=0.429$) where we got higher birefringence for $\eta_i=0.571$.

$$B = |n_x - n_y| \quad (1)$$

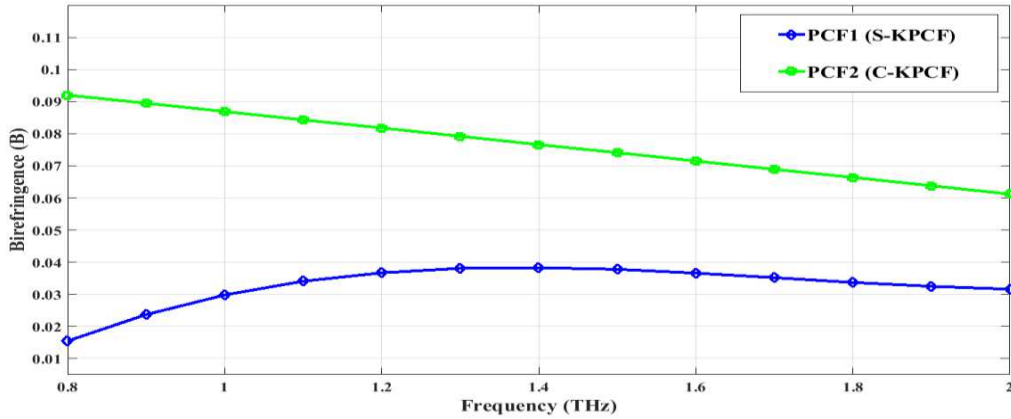


Fig. 3: Birefringence Vs Frequency (THz) for PCF1 (S-KPCF) and PCF2 (C-KPCF).

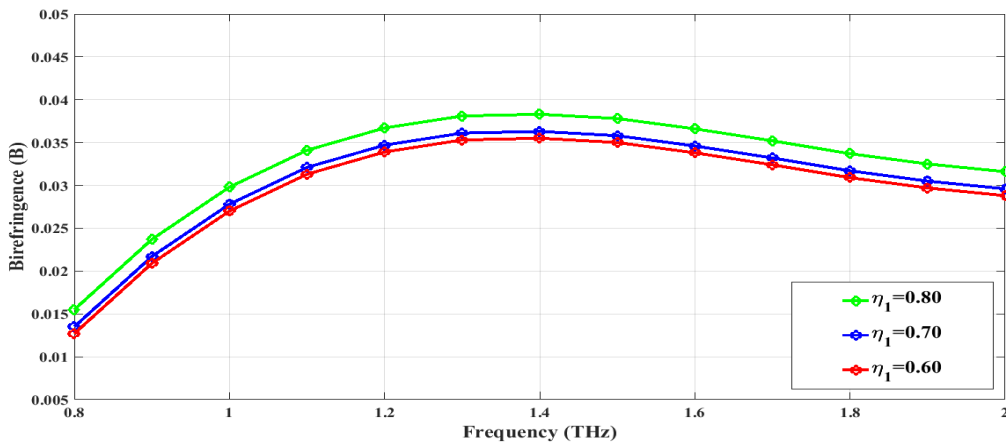


Fig. 4: Birefringence Vs Frequency (THz) for different ratio of η_1 for PCF1.

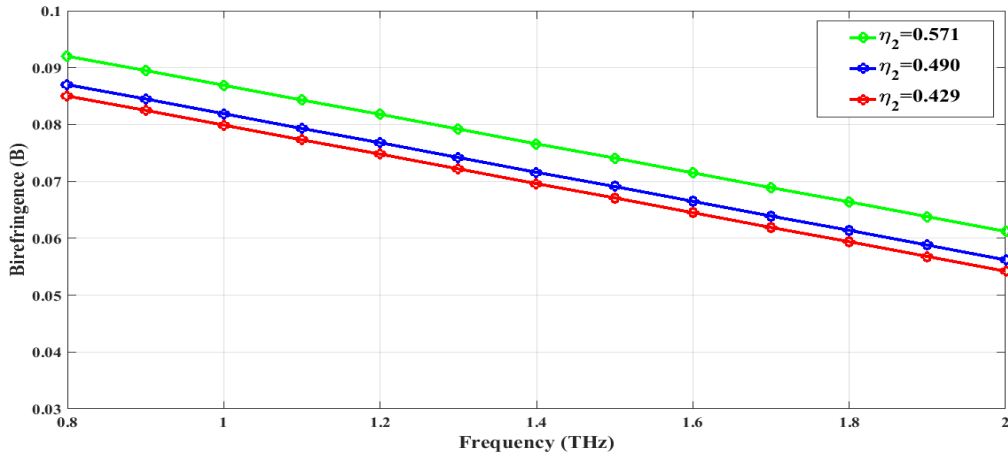


Fig. 5: Birefringence Vs Frequency (THz) for different ratio of η_2 for PCF2.

B) Effective Material Loss (EML)

Eq. (2) shows the equation to calculate EML for the proposed PCFs. Here, ϵ_0 , μ_0 , E , α_{mat} , n , S_z are permittivity in vacuum, permeability in vacuum, Electric field of fundamental mode, bulk material absorption loss, refractive index of background material, pointing vector along z direction respectively. EML curve for proposed PCF1 and PCF2 has been depicted in Fig 6. The figure illustrates that for PCF2 we get lower EML than PCF1. The EML curve for PCF2 is flat and in decreasing mode whereas the curve of PCF1 is slight increasing order from 0.8THz to 1.1THz and then decreasing order from 1.2 THz to 2THz. Fig. 7 depicts the results for the variation of η_1 . From the figure it is clear that for $\eta_1 = 0.60$ we get lower EML for PCF1. For PCF2 we get lower EML for $\eta_2 = 0.429$. Although we get lower EML for $\eta_1 = 0.60$ and $\eta_2 = 0.429$ but to optimize the PCF structures we fixed $\eta_1 = 0.80$ and $\eta_2 = 0.571$ as we get better optical properties.

$$EML = \frac{(\frac{\epsilon_0}{\mu_0})^{1/2} \int_{A_{mat}} n \alpha_{mat} |E|^2 dA}{2 \int_{All} S_z dA} \quad (2)$$

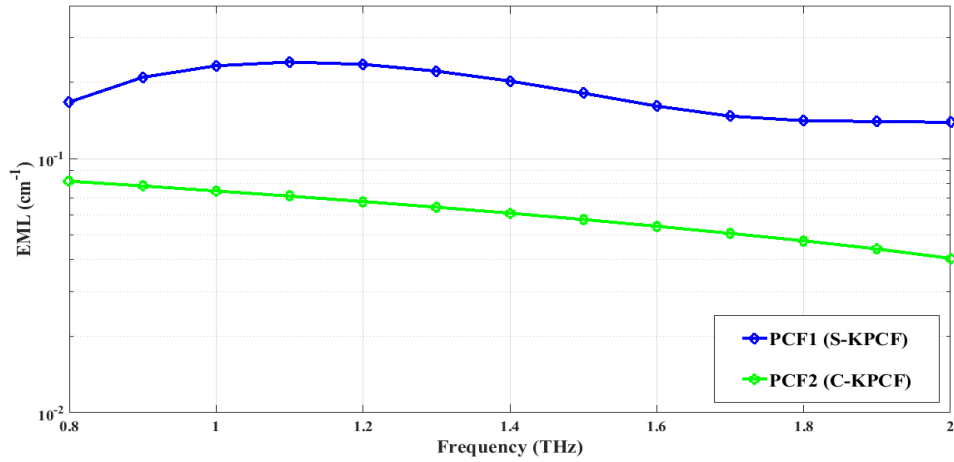


Fig. 6: EML Vs Frequency (THz) for PCF1 (S-KPCF) and PCF2 (C-KPCF).

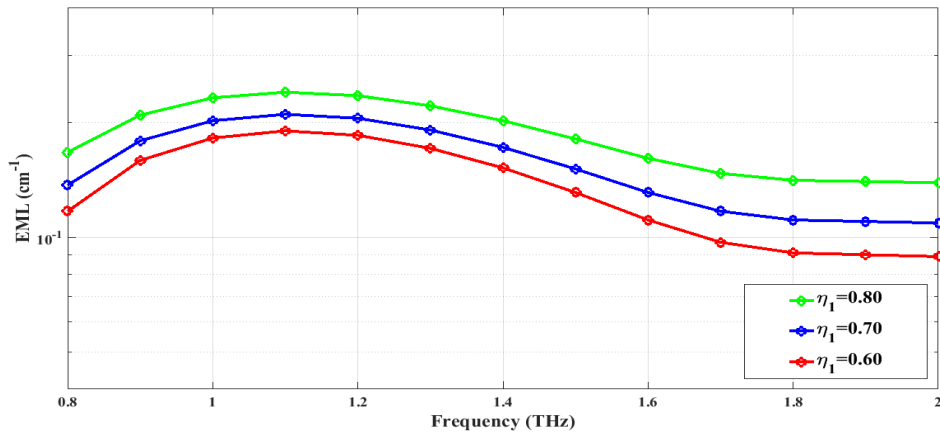


Fig. 7: EML Vs Frequency (THz) for different ratio of η_1 for PCF1.

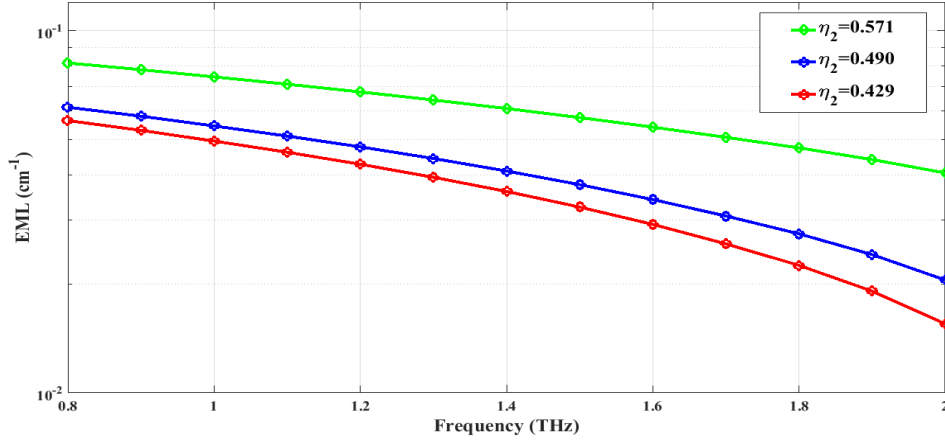


Fig. 8: EML Vs Frequency (THz) for different ratio of η_2 for PCF2.

C) Confinement loss

Confinement loss or leakage loss can be computed by the following equation Eq(3) where f is the operating frequency and $\text{Im}(n_{\text{eff}})$ is the imaginary refractive index of PCFs [17]. Fig 9 illustrates the confinement loss for PCF1 and PCF2 from frequency range 0.8THz to 2THz. The figure shows that for PCF2 (C-KPCF) we get lower confinement loss higher the PCF1 (S-KPCF). For S-KPCF the confinement loss curve diminishes with the change of frequency but not at a constant rate. But for C-KPCF the confinement loss decreases slightly at a constant rate.

$$CL = 8.686 \times \frac{2\pi f}{c} \text{Im}(n_{\text{eff}}) \quad (3)$$

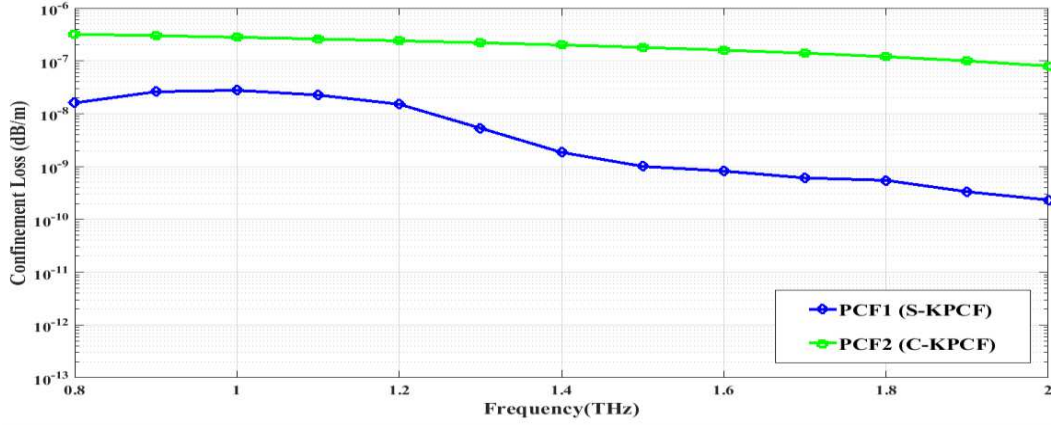


Fig. 9: Confinement loss Vs Frequency (THz) for PCF1 (S-KPCF) and PCF2 (C-KPCF).

D) Bending Loss

Bending loss occurs due to bending of the photonic crystal fiber. Bending loss can be calculated by Eq (4), Eq(5) and Eq(6). Eq (6) is the equation for calculating effective area. In this research we have calculated effective area for both PCFs. $F(x)$ is the function which should be used in Eq (4). In the equation Eq(4) A_{eff} is the effective area, R_b is the bending radius, $\beta = 2\pi n_{\text{co}} / \lambda$ and $\beta_{\text{cl}} = 2\pi n_{\text{cl}} / \lambda$. n_{co} and n_{cl} are refractive index of core and cladding. In this research we have calculated the bending loss of the PCF1 and PCF2 for $R_b = 1\text{cm}$ and $R_b = 2\text{cm}$ which has been shown in Fig 10 and Fig 11. For PCF1 (S-KPCF) we get lower bending loss for $R_b = 2\text{cm}$ shown in Fig 10 and for PCF2(C-KPCF) we get lower bending loss for $R_b = 1\text{cm}$. For both PCFs (S-KPCF and C-KPCF) we got lower bending loss.

$$\alpha_{BL} = \frac{1}{8} \sqrt{\frac{2\pi}{3}} \frac{1}{\beta A_{\text{eff}}} F \left[\frac{2}{3} R_b \frac{(\beta^2 - \beta_{\text{cl}}^2)^{\frac{2}{3}}}{\beta^2} \right] \quad (4)$$

$$F(x) = x^{-\frac{1}{2}} e^{-x} \quad (5)$$

$$A_{\text{eff}} = \frac{[\int I(r) r dr]^2}{[\int I^2(r) dr]^2} \quad (6)$$

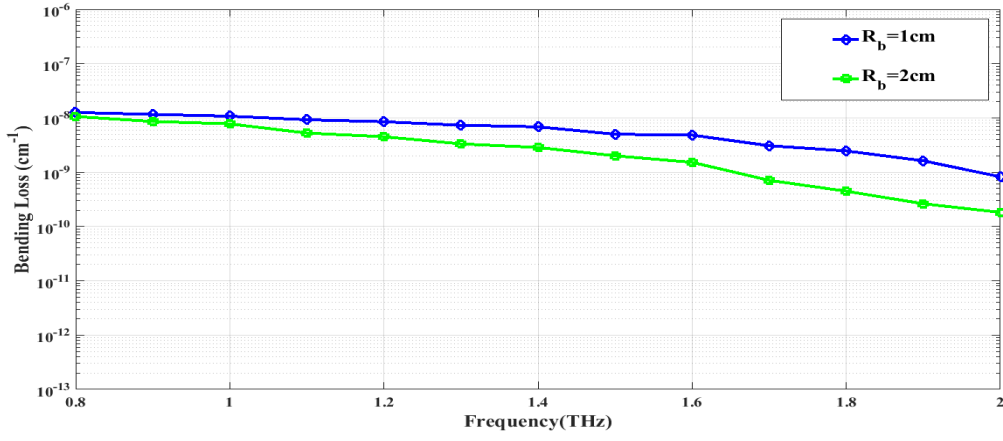


Fig. 10: Bending Loss Vs Frequency (THz) for PCF1 (S-KPCF) with different bending radius.

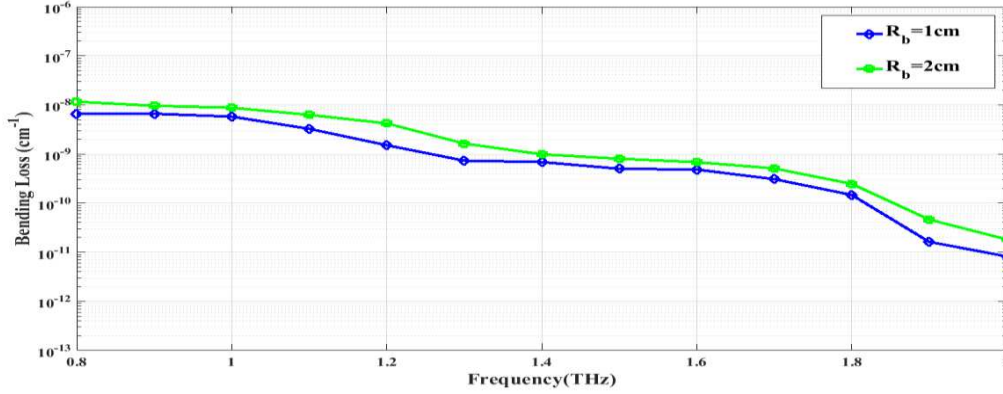


Fig. 11: Bending Loss Vs Frequency (THz) for PCF2 (C-KPCF) with different bending radius.

E) Total Loss

TL=Bending Loss+ EML+ Confinement loss. Total loss can be calculated by summation of Bending loss, Effective Material Loss (EML) and confinement loss. Fig 12 shows the total loss curve for PCF1 and PCF2. For PCF1 (S-KPCF) total loss curve increases from 0.8THz to 1.1THz but decreases upto 1.7 THz and remain linear upto 2THz. For PCF2 (C-KPCF) total loss curve decreases constantly from 0.8THz to 2 THz. The figure illustrates that total loss for PCF2 is lower than PCF1.

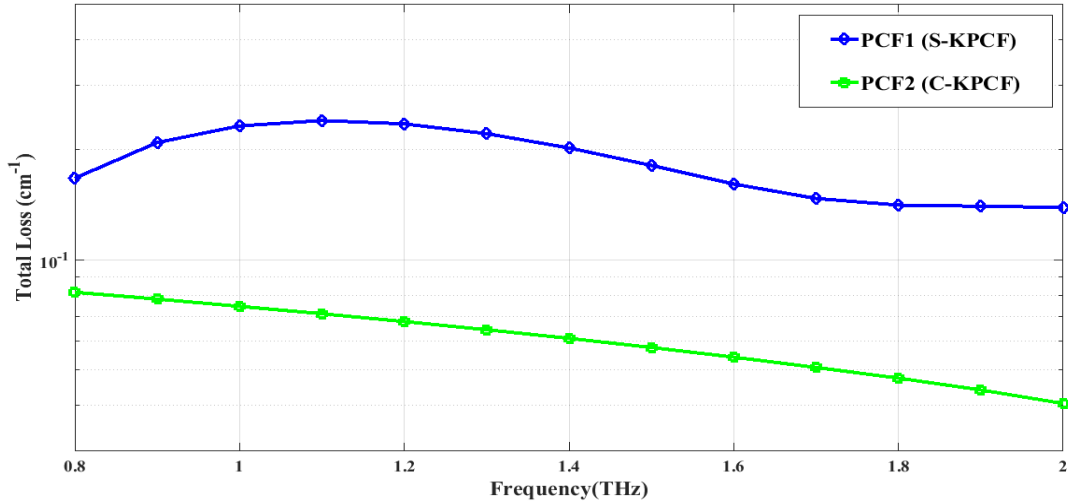


Fig. 12: Total Loss Vs Frequency (THz) for PCF1 (S-KPCF) and PCF2 (C-KPCF).

F) Dispersion

Dispersion of the proposed PCFs can be calculated by Eq (7) where n_{eff} is the effective refractive index of proposed PCFs and $\omega=2\pi f$. Dispersion curve of the proposed PCF1 (S-KPCF) and PCF2 (C-KPCF) along X-Axis and Y-Axis has been shown in Fig 13. The figure describes that for S-KPCF the dispersion curve shows that the values of the dispersion are near zero and almost flat. The C-KPCF dispersion curve is also near zero and flat [18].

$$\beta_2 = \frac{2}{3} \frac{dn_{eff}}{d\omega} + \frac{\omega}{c} \frac{d^2 n_{eff}}{d\omega^2} \quad (7)$$

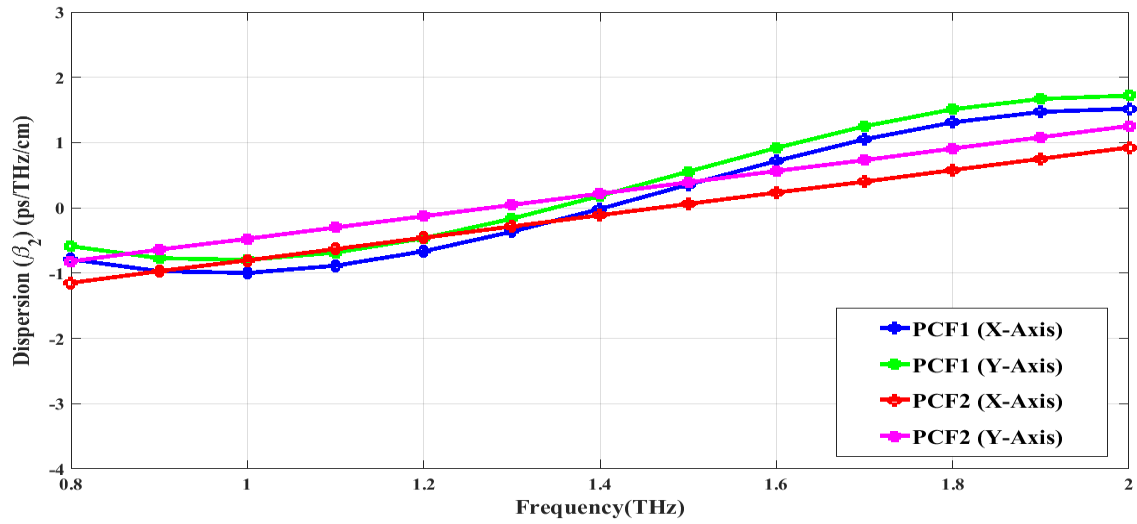


Fig. 13: Dispersion Vs Frequency (THz) for PCF1 and PCF2 along X-Axis and Y-Axis.

G) V-Parameter

V-Parameter is the parameter which can be used for measuring any PCF as it is single mode or multimode. If value of V-parameter is less than 2.405 then it is single mode and if higher then the PCF is multimode. V-parameter equation has been shown in Eq(8) where r is the radius of core region, f is the operating Frequency, n_{co} is the refractive index of core and n_{cl} is the refractive index of cladding. Fig 14 shows that for both of the PCFs V-parameters value increases with the increase of Frequency. From the figure which is clear that both PCFs (PCF1 and PCF2) are multimode fiber.

$$V = \frac{2\pi f}{c} \sqrt{n_{co}^2 - n_{cl}^2} \quad (8)$$

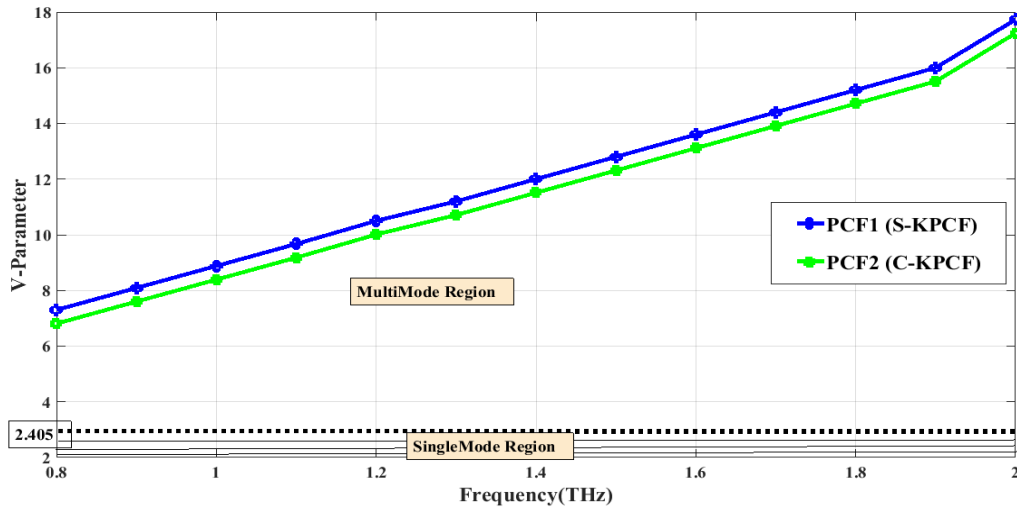


Fig 14: V-Parameter Vs Frequency for PCF1 (S-KPCF) and PCF2 (C-KPCF).

Comparison between the prior PCFs and Proposed PCFs (both PCF1 and PCF2) has been shown in Table 1. Table describes that our proposed two PCFs (PCF1 and PCF2) shows better results in all aspect of optical parameters. In our proposed PCFs different parameters like birefringence, dispersion, EML, confinement loss, total loss, bending loss shows better results at the same time.

Table 1: Comparison between previously published PCF and Proposed PCFs at 1THz

Ref	Birefringence	Confinement loss	EML	Dispersion	Bending Loss	Total Loss	Structure
Proposed PCF1	2.98×10^{-2}	2.76×10^{-8}	0.232	-0.997	10.76×10^{-9}	0.232	Slotted Core Kagome PCF
Proposed PCF2	8.69×10^{-2}	2.98×10^{-7}	0.0746	-0.797	7.76×10^{-9}	0.746	Circular Core Kagome PCF
Prior PCF [19]	-	8.96×10^{-3}	0.0760	0.96 ± 0.086	10^{-2}	0.392	Square Square PCF
Prior PCF [20]	-	0.29	0.12	-	-	1.43	Hexa Hexa PCF
Prior PCF [21]	-	2.05×10^{-3}	0.066	-	-	0.71	Hexa Roated Core PCF
Prior PCF [22]	-	8.4×10^{-4}	0.02227	0.15 ± 0.12	2×10^{-6}	-	Hexagonal PCF

IV. Conclusion

Two novel slotted core Kagome PCF (S-KPCF) and circular core Kagome PCF (C-KPCF) has been depicted in this research. Core of S-KPCF is formed with elliptical and rectangular slots and core of C-KPCF is formed with circular hole in hexagonal shape. As background material of the proposed PCFs TOPAS has been used. HRS materials filled at core region are surrounded by ENZ material of the two PCFs. The two PCF has been compared between them and also compared with previous PCFs. Our proposed PCFs shows higher birefringence, lower total loss, lower confinement loss, low EML, low bending loss simultaneously. The operating frequency is very wide in this investigation for THz regime. V-parameter is calculated as for S-KPCF is 9.77 and for C-KPCF is 8.23 which points that both PCFs are in multimode region. The proposed PCFs (S-KPCF and C-KPCF) also show near zero flat dispersion. The proposed PCFs is suitable for THz wave guidance and it will afford new applications in THz regime.

Funding Acknowledgements: This study was funded by the Deanship of Scientific Research, Taif University Researchers Supporting Project number (TURSP-2020/08), Taif University, Taif, Saudi Arabia.

Data and material/Code Availability: The proposed model is simulated and numerically investigated by simulation software. These data are available from the corresponding author on reasonable request.

Conflict of interest: All the authors approved for submission as well as no competing interests.

REFERENCES

1. Aming, A., Uthman, M., Chitaree, R., Mohammed, W., & Rahman, B. A. (2016). Design and characterization of porous core polarization maintaining photonic crystal fiber for THz guidance. *Journal of Lightwave Technology*, 34(23), 5583-5590.
2. Kaijage, S. F., Ouyang, Z., & Jin, X. (2013). Porous-core photonic crystal fiber for low loss terahertz wave guiding. *IEEE Photonics Technology Letters*, 25(15), 1454-1457.
3. Russell, P. S. J. (2006). Photonic-crystal fibers. *Journal of lightwave technology*, 24(12), 4729-4749.
4. Yang, J., Yang, B., Wang, Z., & Liu, W. (2015). Design of the low-loss wide bandwidth hollow-core terahertz inhibited coupling fibers. *Optics Communications*, 343, 150-156.
5. Sharma, M., Borogohain, N., & Konar, S. (2013). Index guiding photonic crystal fibers with large birefringence and walk-off. *Journal of lightwave technology*, 31(21), 3339-3344.
6. Hassani, A., Dupuis, A., & Skorobogatiy, M. (2008). Porous polymer fibers for low-loss Terahertz guiding. *Optics express*, 16(9), 6340-6351.
7. Kim, S. E., Kim, B. H., Lee, C. G., Lee, S., Oh, K., & Kee, C. S. (2012). Elliptical defected core photonic crystal fiber with high birefringence and negative flattened dispersion. *Optics express*, 20(2), 1385-1391.
8. Yang, T., Ding, C., Ziolkowski, R. W., & Guo, Y. J. (2018). Circular hole ENZ photonic crystal fibers exhibit high birefringence. *Optics express*, 26(13), 17264-17278.
9. Habib, M. S., & Khandker, E. (2015). Highly birefringent photonic crystal fiber with ultra-flattened negative dispersion over S+ C+ L+ U bands. *Applied optics*, 54(10), 2786-2789.
10. Habib, A., Anower, S., & Hasan, R. (2017). Ultrahigh birefringence and extremely low loss slotted-core microstructure fiber in terahertz regime. *Current Optics and Photonics*, 1(6), 567-572.
11. Faisal, M., & Islam, M. S. (2018). Extremely high birefringent terahertz fiber using a suspended elliptic core with slotted airholes. *Applied optics*, 57(13), 3340-3347.
12. Rana, S., Rakin, A. S., Hasan, M. R., Reza, M. S., Leonhardt, R., Abbott, D., & Subbaraman, H. (2018). Low loss and flat dispersion Kagome photonic crystal fiber in the terahertz regime. *Optics Communications*, 410, 452-456.
13. Hasanuzzaman, G. K. M., Rana, S., & Habib, M. S. (2016). A novel low loss, highly birefringent photonic crystal fiber in THz regime. *IEEE Photonics Technology Letters*, 28(8), 899-902.
14. Rana, S., Rakin, A. S., Subbaraman, H., Leonhardt, R., & Abbott, D. (2017). Low loss and low dispersion fiber for transmission applications in the terahertz regime. *IEEE Photonics Technology Letters*, 29(10), 830-833.
15. Yang, T., Wang, E., Jiang, H., Hu, Z., & Xie, K. (2015). High birefringence photonic crystal fiber with high nonlinearity and low confinement loss. *Optics express*, 23(7), 8329-8337.
16. Islam, R., Habib, M. S., Hasanuzzaman, G. K. M., Rana, S., & Sadath, M. A. (2016). Novel porous fiber based on dual-asymmetry for low-loss polarization maintaining THz wave guidance. *Optics letters*, 41(3), 440-443.
17. Yang, T., Ding, C., Ziolkowski, R. W., & Guo, Y. J. (2018). Circular hole ENZ photonic crystal fibers exhibit high birefringence. *Optics express*, 26(13), 17264-17278.
18. Hossain, M. S., Razzak, S. A., Markos, C., Hai, N. H., Habib, M. S., & Habib, M. S. (2020). Highly Birefringent, Low-Loss, and Near-Zero Flat Dispersion ENZ Based THz Photonic Crystal Fibers. *IEEE Photonics Journal*, 12(3), 1-9.
19. Hasan, M. R., Islam, M. A., & Rifat, A. A. (2016). A single mode porous-core square lattice photonic crystal fiber for THz wave propagation. *Journal of the European Optical Society-Rapid Publications*, 12(1), 1-8.
20. Uthman, M., Rahman, B. M. A., Kejalakshmy, N., Agrawal, A., & Grattan, K. T. V. (2012). Design and characterization of low-loss porous-core photonic crystal fiber. *IEEE Photonics Journal*, 4(6), 2315-2325.
21. Islam, R., Hasanuzzaman, G. K. M., Habib, M. S., Rana, S., & Khan, M. A. G. (2015). Low-loss rotated porous core hexagonal single-mode fiber in THz regime. *Optical Fiber Technology*, 24, 38-43.

22. Islam, M. S., Faisal, M., & Razzak, S. A. (2017). Dispersion flattened porous-core honeycomb lattice terahertz fiber for ultra low loss transmission. *IEEE Journal of Quantum Electronics*, 53(6), 1-8.